

Simulation Techniques for Susceptibility Optimisation of Field Probes

Wieland A. Worthoff¹, Stefan Schwan¹, Johannes Lindemeyer¹, and N. Jon Shah^{1,2}

¹Institute of Neuroscience and Medicine, Forschungszentrum Jülich GmbH, Jülich, Germany, ²Faculty of Medicine, Department of Neurology, RWTH Aachen University, JARA, Aachen, Germany

TARGET AUDIENCE – Physicists, engineers, researchers requiring field sensing and monitoring devices.

PURPOSE – Magnetic resonance field sensors have been used for a broad range of applications, including post-processing correction of MRI data¹, real-time shimming², and correction of subject motion³. Measurements of the magnetic field also provide means of examining⁴ and optimizing pulse sequences. To optimise field probe design in particular with respect to its own susceptibility distribution as well as its surrounding magnetic environment, a simulation algorithm is used, which was originally used to predict the susceptibility-induced field in the human head.

METHODS – A field probe consists of an NMR active sample droplet inside a capillary with a solenoidal micro-coil fixed concentrically around the outside. The droplet is surrounded by a matched buffer fluid⁵, D₂O + MnCl₂ (figure 1) and is sealed using glass plugs to avoid the formation of bubbles and prevent movement of the droplet. The entire field probe can be immersed in epoxy⁵. 3D models of the field probe components are transformed into a mesh of discrete susceptibility voxels and are used as input of a simulation based on a Fourier-approach⁶ to determine the local magnetic field from dipolar field contributions due to the susceptibility of structures in the vicinity of the sample droplet. The simulation operates on a mesh size of 256x192x320 to simulate a region of interest (ROI) of 10x7.5x20 mm³ and assumes an infinitely long capillary and an infinite body of air as the far-distant environment of the probe. The local field distributions within the NMR-active sample droplet are analysed.

Field probes are commonly deployed in confined locations and in close vicinity to foreign objects. Such objects might be the housing, scanner components or the subject itself. All of these are objects of potentially unmatched susceptibility, which influence the performance of the field probe. In particular these objects lack any symmetry. The case in which such an object is located in the near vicinity of a field probe is simulated by means of introducing an object as a 3D model to the simulation space. The distance between the object and the field probe is then varied and the distribution of magnetic field values is analysed. Furthermore, in order to investigate the effects of technical imperfections concerning the matched liquid buffer, we simulate field probes with different buffer fluid susceptibility and buffer volume. The susceptibility of MnCl₂ doped D₂O is determined via detection of the phase disturbance in water surrounding a sample tube containing D₂O with different dopant concentrations, employing a minimization approach based on forward dipole convolution^{6,7}. The model is verified against experiments on a 9.4T MRI system. The field probes use 2.2 mm³ cyclohexane as active medium, using different length of buffers made of MnCl₂ doped D₂O, with varying dopant concentrations. The capillaries have a 4 mm outer diameter and 0.8 mm inner diameter. The probes are positioned at a fixed location within the scanner bore, free induction decays are acquired and their spectrum is analysed and compared to the output of the simulation.

RESULTS – A sphere of water with a magnetic susceptibility of -9.01×10^{-6} and a diameter of 2 mm is positioned on the z-axis at distances d away from the field probe (distance centre of sample droplet to centre of sphere). Figure 2 shows contour colour plots of the field distribution as well as the corresponding histograms for $d = 3.5$ mm and 7.5 mm. The field generated by the sphere perturbs the field distribution within the droplet, causing a broadening and change in the histogram, thus distorting the NMR peak. This effect is similar to what is observed in an experiment, where a field probe is positioned at the centre of the magnet with a water phantom placed in near vicinity of the probe. The peak shape is distorted and only regains its unperturbed line shape once the sphere is located further away. Figure 3 is a plot of the width of 100 simulated histogram data sets corresponding to linear increments of d over the interval from 3.5 mm to 7.5 mm. For comparison, two spectra for $d = 3$ mm and 7 mm are shown in the inset, these compare to what is predicted by the simulation.

DISCUSSION – Analysing susceptibility effects numerically is beneficial to the process of building high sensitivity field monitoring devices. The demonstrated algorithm is verified by experiment to predict successfully the impact of buffer liquid dopant concentration and can be used to determine minimum buffer volumes. Furthermore it is demonstrated and experimentally validated, how the field probe environment can be included in the simulation in order to predict its influence on a field probe measurement.

The buffer fluid has a great impact on field probe signal fidelity, as the proper matching avoids an inhomogeneous field distribution inside the droplet. Understanding the results of slight variation in susceptibility compared to other susceptibility effects within the probe can optimise the design process significantly.

CONCLUSION – The simulation technique provides a novel way to assess information about the field distribution within the sample droplet. The simulation gives comparable results to experiment. We intend to use this information to further optimize the geometry of our field probe design and positioning of the field probes

ACKNOWLEDGMENTS – The authors gratefully thank Michael Poole, Nadine Rosen and Arthur Magill.

REFERENCES – 1. Barmet, C. et al., MRM 2008;60:187–197. 2. Van Der Velden, T. A. et al., MAGMA 2013; 26(1):73. 3. Haeberlin, M. et al., Proc. Intl. Soc. Mag. Reson. Med. 2012;20:595. 4. Dietrich, B. E. et al., Proc. Intl. Soc. Mag. Reson. Med. 2011;19:1842. 5. De Zanche, N. et al., Magn Reson Med, 60:176–186 (2008) 6. Marques, J. P. and Bowtell, R., Concept. Magn. Reson. B. 2005;25B(1):65–78. 7. Koch, K. M. et al., PMB 2006, 51(24), 6381–402.

Fig. 1 Geometry of a field probe and an object in its vicinity.

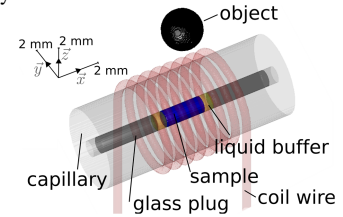


Fig. 2 A sphere at a distance d perturbs the magnetic field distribution within the droplet: colormaps of the field distribution in the ROI (a), inside the droplet (b) and the corresponding magnetic field distributions (c).

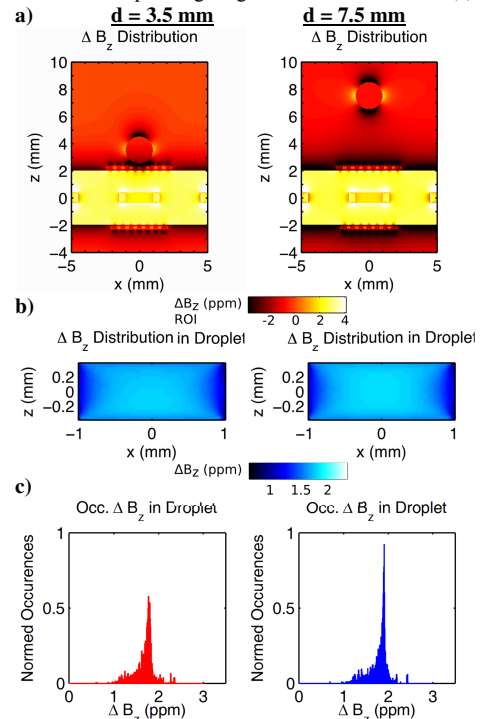


Fig. 3 Comparison of simulation and experimental data.

